Space-Time Curvature of Unusual Metrics
Junior Independent Study: Self Design Project

Min Sung Kim
Physics Department, The College of Wooster, Wooster, Ohio 44691, USA
(Dated: April 26, 2013)

This research is an attempt to further develop cloaking through the stress energy momentum that has been studied in College of Wooster physics department, by specifically exploring the behaviors of swirling space-time. A program was developed, which calculates a specific space-time geometry according to the given metric. The strength of this program is that it accepts any diagonally symmetric metric. However, there is the downfall of such general input, as it only provides mathematical boundaries, disregarding physical boundaries. Moreover, the visualizations that were generated have their limits in specifying what exactly is happening. Randomly generated metrics were put through the programs, which lead to a very unusual space-time curvature. However, unfortunately, attempts to further understand only lead us to incomprehensible results.

I. INTRODUCTION

Sir Isaac Newton developed the law of universal gravitation,

$$F = G\frac{m_1 m_2}{r^2}, \tag{1}$$

in the 17th century, in order to better understand the motion triggered by the attraction between two masses. His law was successful in describing the motion at low speeds. However, his theory of gravitation is not able to explain the source of such attraction nor other general relativistic effects.

Studying electromagnetism, Albert Einstein realized that the Newtonian mechanics clashed with the laws of the electromagnetic fields [2]. He developed the special theory of relativity, which was expanded to explain gravitational fields. By 1915, Albert Einstein developed a theory of gravity named general relativity, taking another step to truly understanding the source of gravity and its effects. Einstein's relativity has been congruent to the vast majority of recent discoveries and experiments and has been used to further develop the theories of natural phenomena. The conjoining of general relativity and electromagnetism lead physicists to develop the relativistic quantum field theory in mid 20th century.

In this experiment, I was able to use general relativity to create a program that will generate visualizations of manipulated space times. Through the program, elements that develops the geometry of the space-time is manipulated as an attempt to better understand the role of each element in determining the space-time curvature.

II. THEORY

A. Coordinates

The notation for the space-time coordinates in general relativity can be reduced to x^μ, where

$$x^\mu \leftrightarrow \begin{bmatrix} x^0 \\ x^1 \\ x^2 \\ x^3 \end{bmatrix} = \begin{bmatrix} ct \\ x \\ y \\ z \end{bmatrix}. \tag{2}$$

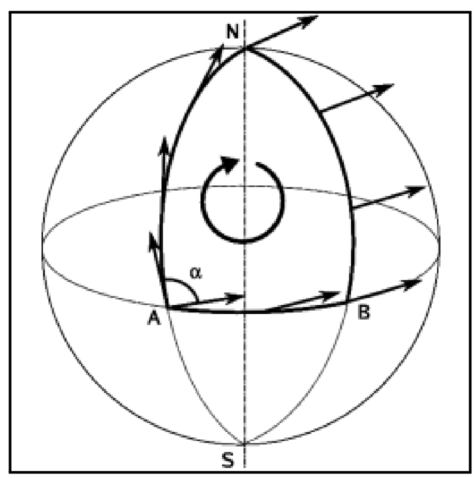

FIG. 1: Visualization of a parallel vector transportation on a curved surface. Starting from point A, the vector is transported to point N, B, then back to A. The vector does not match after the transportation around the curved surface, as it would on a flat surface.

The Greek letter indices can be expanded from zero to three, where each number represents a variable of a dimension; x^0 is the time dimension, and x^1, x^2, and x^3 are the spatial dimensions. The notation applies similarly for the spherical coordinates, as

$$x^\mu \leftrightarrow \begin{bmatrix} x^0 \\ x^1 \\ x^2 \\ x^3 \end{bmatrix} = \begin{bmatrix} ct \\ r \\ \phi \\ \theta \end{bmatrix}. \tag{3}$$

B. The Metric

Neither the length nor time intervals are absolute in general relativity, but there are invariant constants that do not depend on the reference frame [1]. The quantity of these invariants are four-dimensional "distance" separation. An invariant section of a space time is denoted by $d\sigma$. The Riemannian metric allows us to create the connection, which is quadratic[1], as

$$d\sigma^2 = \sum_{\mu=0}^{3}\sum_{\nu=0}^{3} g_{\mu\nu} dx^\mu dx^\nu. \tag{4}$$

$g^{\mu\nu}$ implies summation between the repeated indices on following pair of dx. Often, even if the Einstein summation notation is not specified, such summations over repeated indices are always implied. In rectangular coordinates, the flat space time metric is

$$g_{\mu\nu} = \eta_{\mu\nu} \leftrightarrow \begin{bmatrix} -1 & 0 & 0 & 0 \\ 0 & 1 & 0 & 0 \\ 0 & 0 & 1 & 0 \\ 0 & 0 & 0 & 1 \end{bmatrix}, \tag{5}$$

which is often called the Minkowski metric; in spherical coordinates, the flat space-time metric is

$$g_{\mu\nu} = \eta_{\mu\nu} \leftrightarrow \begin{bmatrix} -1 & 0 & 0 & 0 \\ 0 & 1 & 0 & 0 \\ 0 & 0 & r^2 & 0 \\ 0 & 0 & 0 & r^2 \sin^2\theta \end{bmatrix}. \tag{6}$$

The time dimension have the opposite sign of the spatial dimensions. In this particular convention, the time dimension is negative, and the spatial dimensions are positive. Note that

$$g^{\mu\nu} = g^{\nu\mu}, \tag{7}$$

requiring that the metric must be symmetric along the diagonal elements.

C. Connection & Curvature

In curved space-time, the components of a vector does not retain as shown in Fig. 1. The connection coefficient or the Riemannian metric, Γ, allow us to calculate the change in components of a vector. A comma signifies a differentiation in respect to the index that follows, such as

$$A^\mu_{,\nu} = \frac{dA^\mu}{dx^\nu}. \tag{8}$$

The connection coefficient is given as

$$\Gamma_{\mu\nu\sigma} = \frac{1}{2}(g_{\mu\nu,\sigma} + g_{\sigma\mu,\nu} - g_{\nu\sigma,\mu}). \tag{9}$$

Indices can be raised or lowered using the metric, as

$$g^{\mu\alpha}\Gamma_{\alpha\nu\sigma} = \Gamma^\mu_{\nu\sigma}. \tag{10}$$

D. Ricci Tensor and the Einstein Curvature Tensor

The Ricci Curvature tensor, R, allows us to measure the degree of which the Riemannian metric affects the curvature of space-time. Binding of lower indices for Riemann and Ricci tensor (shown in Eq. 11) allows us to develop the Einstein curvature tensor, G, through which we can compute the curvature of the space-time. The Ricci Tensor can be written using the connection coefficients;

$$R^\mu_{\nu\sigma\alpha} = \Gamma^\mu_{\nu\alpha,\sigma} - \Gamma^\mu_{\nu\sigma,\alpha} + \Gamma^\rho_{\nu\alpha}\Gamma^\mu_{\rho\sigma} - \Gamma^\rho_{\nu\sigma}\Gamma^\mu_{\rho\alpha} \tag{11}$$

The Ricci tensor can be contracted as

$$R_{\mu\nu} = R^\alpha_{\mu\nu\alpha}. \tag{12}$$

Furthermore,

$$R = R^\mu_\mu. \tag{13}$$

The reverse trace of the Ricci tensor gives us the Einstein tensor,

$$G^{\mu\nu} = R^{\mu\nu} - \frac{1}{2}R\ g^{\mu\nu}. \tag{14}$$

All of the tensor calculations and metric manipulations are included in Appendix A.

E. Stress Energy Momentum

In general relativity, a particle with a mass is understood as the source of gravitation by curving the space-time around it, and hence "Stress energy momentum can be thought of as the relativistic generalization of mass" [5]. A particle's 4-momentum can be recorded using,

$$p^\mu \leftrightarrow \begin{bmatrix} p^0 \\ p^1 \\ p^2 \\ p^3 \end{bmatrix} = \begin{bmatrix} E \\ p^x \\ p^y \\ p^z \end{bmatrix}. \tag{15}$$

p^0 is the energy of the particle, and the rest are spatial momentum. The stress energy momentum tensor is related to a particle's 4-momentum per unit 3-Volume;

$$T^{\mu\nu} \leftrightarrow \frac{dp^\mu}{d^3V_\nu} \leftrightarrow \begin{bmatrix} \frac{dE}{dx\ dy\ dz} & \frac{dE}{dt\ dy\ dz} & \frac{dE}{dt\ dx\ dz} & \frac{dE}{dt\ dx\ dy} \\ \frac{dp^x}{dx\ dy\ dz} & \frac{dp^x}{dt\ dy\ dz} & \frac{dp^x}{dt\ dx\ dz} & \frac{dp^x}{dt\ dx\ dy} \\ \frac{dp^y}{dx\ dy\ dz} & \frac{dp^y}{dt\ dy\ dz} & \frac{dp^y}{dt\ dx\ dz} & \frac{dp^y}{dt\ dx\ dy} \\ \frac{dp^z}{dx\ dy\ dz} & \frac{dp^z}{dt\ dy\ dz} & \frac{dp^z}{dt\ dx\ dz} & \frac{dp^z}{dt\ dx\ dy} \end{bmatrix}. \tag{16}$$

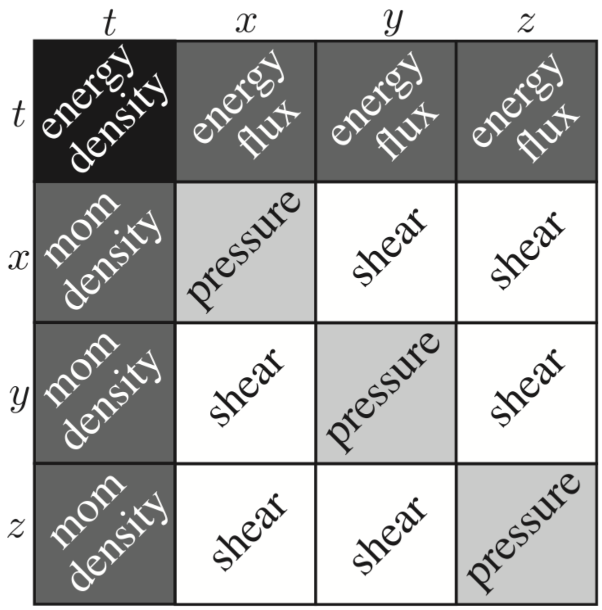

FIG. 2: The plot of stress energy momentum [3]. Notice the pattern regarding energy density/flux, pressure, and shear, within the metric. (rectangular coordinates)

After the conversion to a fraction of force per unit 3-dimension,

$$T^{\mu\nu} \leftrightarrow \begin{bmatrix} \frac{dE}{dV} & \frac{dE}{dt\ dA_x} & \frac{dE}{dt\ dA_y} & \frac{dE}{dt\ dA_z} \\ \frac{dp^x}{dV} & \frac{dp^x}{dA_x} & \frac{dp^x}{dA_y} & \frac{dp^x}{dA_z} \\ \frac{dp^y}{dV} & \frac{dp^y}{dA_x} & \frac{dp^y}{dA_y} & \frac{dp^y}{dA_z} \\ \frac{dp^z}{dV} & \frac{dp^z}{dA_x} & \frac{dp^z}{dA_y} & \frac{dp^z}{dA_z} \end{bmatrix}. \tag{17}$$

Each element corresponds to the stress energy momentum as shown in Fig. 2. Notice that since $T^{\mu\nu}$ is diagonally symmetric within the spatial elements, giving us ten independent equations.

The Einstein field equations in relation to the stress energy momentum tensor is

$$T^{\mu\nu} = \frac{1}{8\pi} G^{\mu\nu}. \tag{18}$$

Because of the stress energy momentum tensor's symmetry within spatial elements, the Einstein tensor must have the same symmetry.

F. Geodesics

In general relativity, a geodesic equation describes a curved space-time, where its tangent vectors are parallel, even after being transported [1]. The law of motion in general relativity is

$$\frac{d^2 x^\mu}{d\tau^2} + \mathit{\Gamma}^\mu_{\alpha\beta} \frac{dx^\alpha}{d\tau} \frac{dx^\delta}{d\tau} = 0, \tag{19}$$

which is the general form of Newton's first law in classical mechanics. The connection coefficient, $\mathit{\Gamma}$ allows us to consider the curvature of space-time. The parameter τ is the proper time. If $v << c$, the connection coefficient goes to zero. Notice that if the connection coefficient becomes zero, Eq. 19 becomes the law of inertia [5];

$$\frac{dv^k}{dt} = 0. \tag{20}$$

The greek index is switched to a latin index, which goes from one to three, only considering the spatial dimensions.

G. The Schwarzschild Metric

One of the most commonly found solution to the Einstein equation is the Schwarzschild metric. It describes the space-time curvature around a spherical mass. The Schwarzschild metric is

$$g_{\mu\nu} \leftrightarrow \begin{bmatrix} -(1 - r_s/r) & 0 & 0 & 0 \\ 0 & (1 - r_s/r)^{-1} & 0 & 0 \\ 0 & 0 & r^2 & 0 \\ 0 & 0 & 0 & r^2 \sin^2\theta \end{bmatrix}. \tag{21}$$

r_s is the Schwarzschild radius, which is the radius of a spherical orbit around the mass that requires the speed of light as the escape speed.

H. The Kerr Metric

Another commonly found solution to the Einstein equation is the Kerr metric. The Kerr metric,

$$g_{\mu\nu} \leftrightarrow$$

$$\begin{bmatrix} c(1 - \frac{r_s r}{\rho^2}) & 0 & 0 & c\frac{2r_s r\alpha \sin^2\theta}{\rho^2} \\ 0 & \frac{-\rho^2}{\mathit{\Delta}} & 0 & 0 \\ 0 & 0 & -\rho^2 & 0 \\ c\frac{2r_s r\alpha \sin^2\theta}{\rho^2} & 0 & 0 & -\left(r^2 + \alpha + \frac{r_s r\alpha^2}{\rho}\sin^2\theta\right)\sin^2\theta \end{bmatrix}, \tag{22}$$

describes the space time around an empty black hole, with a spherical event horizon [2]. Notice the off-diagonal elements within the metric, allowing rotation of space-times. Eq. 22 is true where

$$\rho = \sqrt{r^2 + \alpha^2 \cos(\theta)^2}, \tag{23}$$

$$\mathit{\Delta} = r^2 - r_s r + \alpha^2, \tag{24}$$

and

$$\alpha = \frac{J}{M}; \tag{25}$$

J is the angular momentum of the space-time, and M is the vicinity of a mass [1].

III. PROCEDURE

Mathematica 9 is used to create the program to compute the manipulated space-time geometry and create visualizations. The program for connection was written referencing the program of Syne Salem's independent study [5]. Moreover, the program for geodesic equations was written referencing Duncan Price's Mathematica file [4] from his 2012 summer research.

The parameters within the program are simplified; the gravitational constant, G, and the speed of light, c are reduced to 1. To allow the space-time to swirl in the program, the spherical coordinates are used; Eq. 3.

I was able to create a program that will visualize the manipulated space-time for any kind of metric entered, although they must be symmetric along the diagonal due Eq. 7. Into the manipulated space-time, a bundle of parallel light-like rays are entered, traveling through the space-time. The path of the light rays are plotted, creating a visualization that allows better understanding of the geometry of the space-time.

Through the program, the major metrics are plotted; Minkowski, Schwarzschild, and Kerr. Since the program is able to plot any diagonally symmetric 4×4 metric, versions of the three major metrics and more are also plotted. In an attempt to understand how each element of the metric affects the space time, they are manipulated separately.

IV. RESULTS & ANALYSIS

The program was successfully developed, plotting the space time curvature of any diagonally symmetric metric inputs, and at the same time, recording the path of a bundle of rays to visualize the curvature. As examples, the flat space-time, Schwarzschild and the Kerr metric are discussed in following sections. In all visualizations, the light rays enter from the $+x$ direction. Each metric is visualized in 2 dimensions and 3 dimensions. The 2 dimension visualizations are x and y cross section, where $z = 0$. In 3D visualizations, the axis and ticks are trivial, since the direction of entrance nor the quantity are significant.

A. Flat Space-Time

The flat space-time 2-D visualization is included in Fig. 3 and the 3-D in Fig. 4. From Fig. 3, one can see that light travels straight in flat space-time. However, from Fig. 4, one can notice that the light rays are not quite parallel even though they are traveling in flat space-time. One possible cause is the working precision of the program (which can be increased, compensating with the calculation time), but it is minor, insignificant to the general understanding of the behavior of the space-time within the big picture.

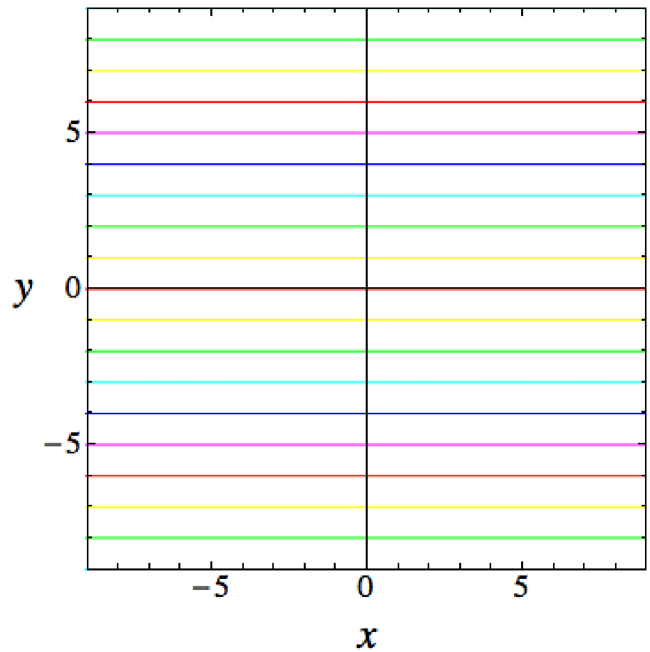

FIG. 3: 2-Dimensional plot of flat space time. The light rays enter the space-time from the $+x$ direction

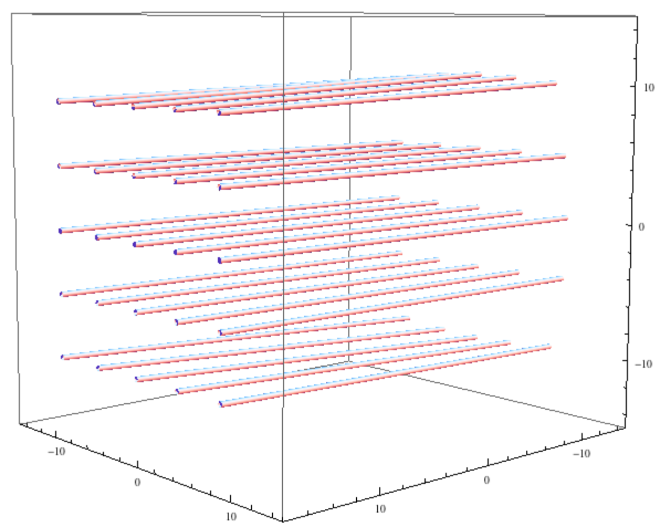

FIG. 4: 3-Dimensional plot of flat space time. The parallel light rays enter from the surface on the left-front side and exit to the opposite side. Notice that the the top layer of rays exit slightly off parallel.

B. The Schwarzschild Metric

The Schwarzschild metric, given in Eq. 21, is put into the program and the respective space-time curvature is visualized in Fig. 5 and Fig. 6; 2-D and 3-D respectively.

In Fig. 5, notice that the rays within the radius (inner most red, yellow, and green rays) of the event horizon

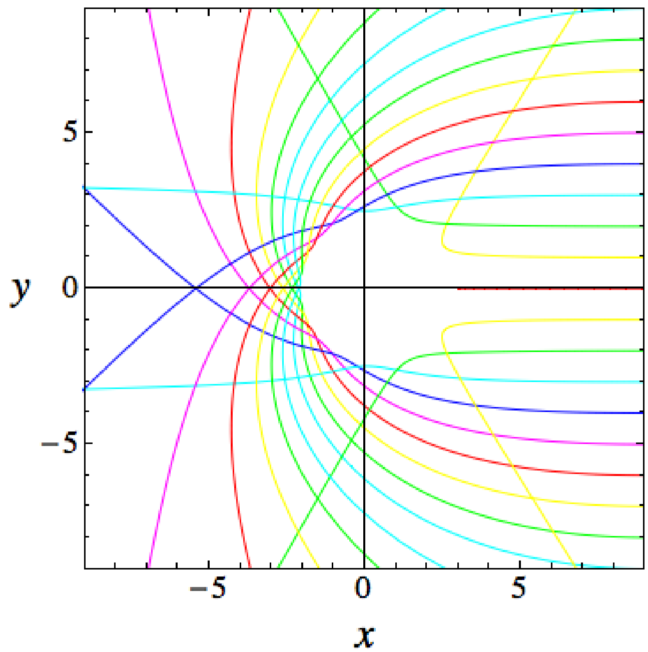

FIG. 5: 2-Dimensional plot of the space-time given by the Schwarzschild Metric.

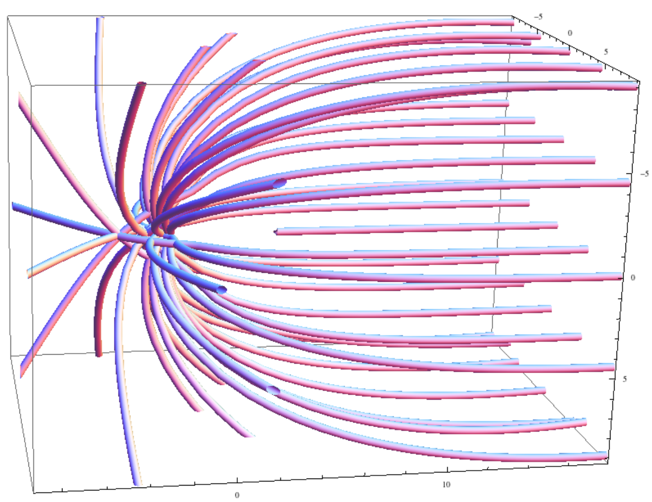

FIG. 6: 3-Dimensional plot of the space-time given by the Schwarzschild Metric.

creates an erroneous results as they enter the boundary. Now, consider Fig. 6, the 3-D visualization; the curvature of space-time around a sphere should also resemble the curvature of the around the sphere. However, remember that the plots only convey the path of the parallel light rays entering from one side, causing Fig. 6 to appear the way it does, only conveying the curvature on the further side of the origin of the light rays.

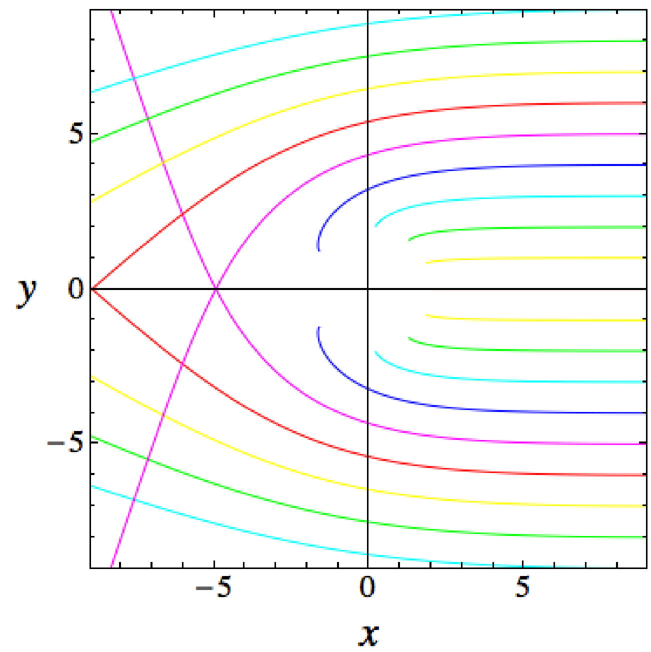

FIG. 7: 2-Dimensional plot of the space-time given by the Kerr Metric. The light rays vanish at the event horizon.

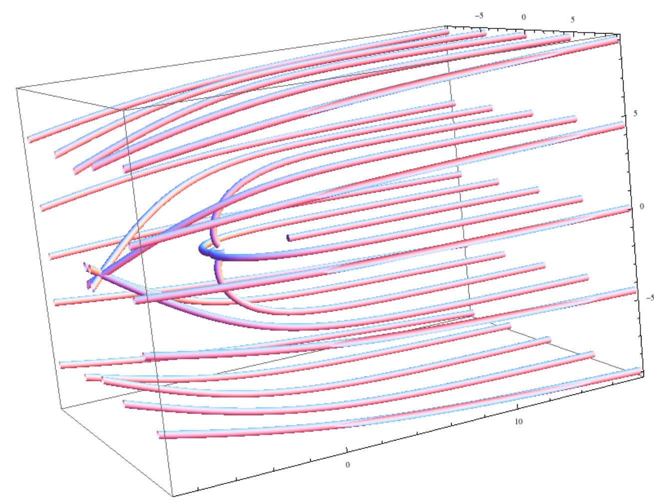

FIG. 8: 3-Dimensional plot of the space-time given by the Kerr Metric. The parallel light rays enter from the surface on the right side. The light rays vanish at the event horizon.

C. The Kerr Metric

The Kerr metric, given in Eq. 22, is put in to the program, and the 2-D visualization is included in Fig. 7, and 3-D in Fig. 8. These visualizations represent a very basic form of a black hole. Notice in both plots that near the center, the light rays suddenly vanish. This signifies that the light rays have entered the event horizon, or the point of no return.

The Kerr Metric allows swirling of the space-time

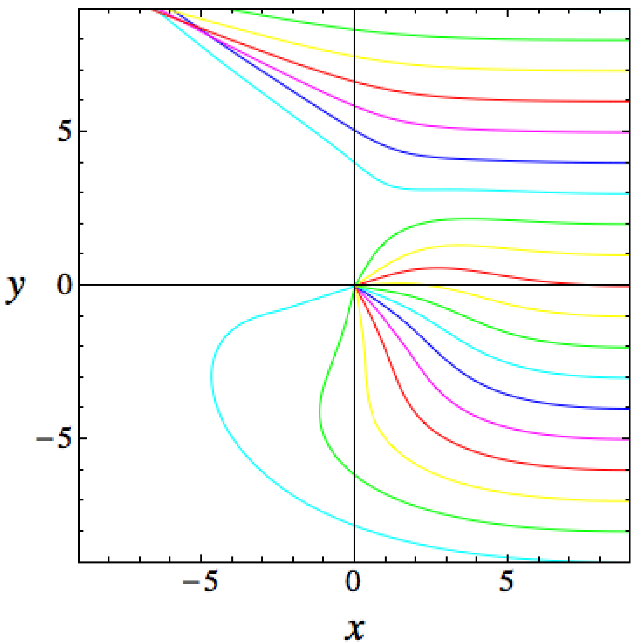

FIG. 9: 2-Dimensional plot of the space-time given by the Kerr Metric with counterclockwise spin (J=2). The parallel light rays enter from the surface on the right side.

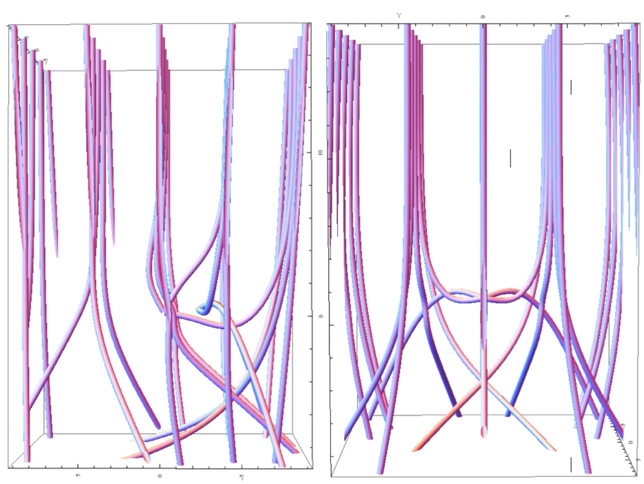

FIG. 10: 3-Dimensional plots of the space-time given by the Kerr Metric with a spin where J=2. The perspective of the plot on the left is $+z$, and right is $+y$. The parallel light rays enter from the top.

around the black hole, as Eq. 22 has off diagonal components, $r\phi$. Fig. 9 is a visualization of a swirling space-time curvature around a black hole in 2-D. The angular momentum of the black hole is in $+\phi$ direction (counter-clockwise).

Fig. 10 is a combined visualization of a swirling space-time curvature around a black hole in 3-D, shown from two different perspectives.

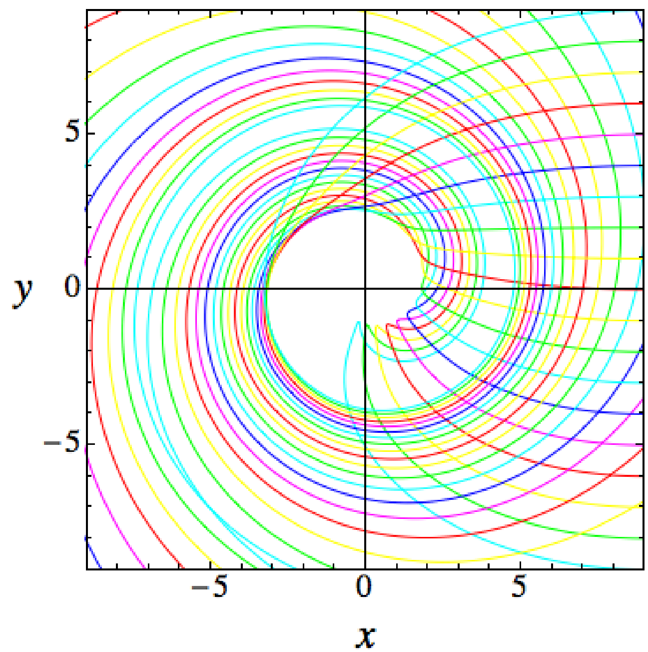

FIG. 11: 2-Dimensional plots of the space-time given by the manipulated Kerr Metric with an angular momentum; J=2; Eq. 26. The parallel light rays enter from the left.

D. Manipulated Kerr Metric

To explore the metric, the Kerr Metric was manipulated randomly. The metric that created an interesting, and possibly non-trivial space-time was the metric which was developed by introducing a $dtdr$ element, $-r\sin\theta$ to the Kerr metric;

$$g_{\mu\nu} \leftrightarrow$$

$$\begin{bmatrix} c(1-\frac{r_s r}{\rho^2}) & -r\sin\theta & 0 & c\frac{2r_s r\alpha\sin^2\theta}{\rho^2} \\ -r\sin\theta & \frac{-\rho^2}{\Delta} & 0 & 0 \\ 0 & 0 & -\rho^2 & 0 \\ c\frac{2r_s r\alpha\sin^2\theta}{\rho^2} & 0 & 0 & \left[r^2+\alpha+\frac{r_s r\alpha^2}{\rho}\sin^2\theta\right]\sin^2\theta \end{bmatrix}. \tag{26}$$

Fig. 11 (2-D) and Fig. 12 (3-D) shows the behavior of the light rays in the manipulated space-time based on Eq. 26.

Consider Fig. 11; it seems that from a distance, the rays travel towards the center of the space-time, but ultimately spin out counter clockwise. Moreover, rays entering from higher values of y have much smoother curvature than that of rays that enter from lower values of y as they are spitted out, since rays that enter from lower values of y initially travel towards the center curving clockwise. Rays that enter from lower values of y, curving clockwise, must counter interact with the counterclockwise spin of the space-time, allowing the light to travel a little closer to the center. Lastly, notice that no light rays on the horizon are able to reach the center.

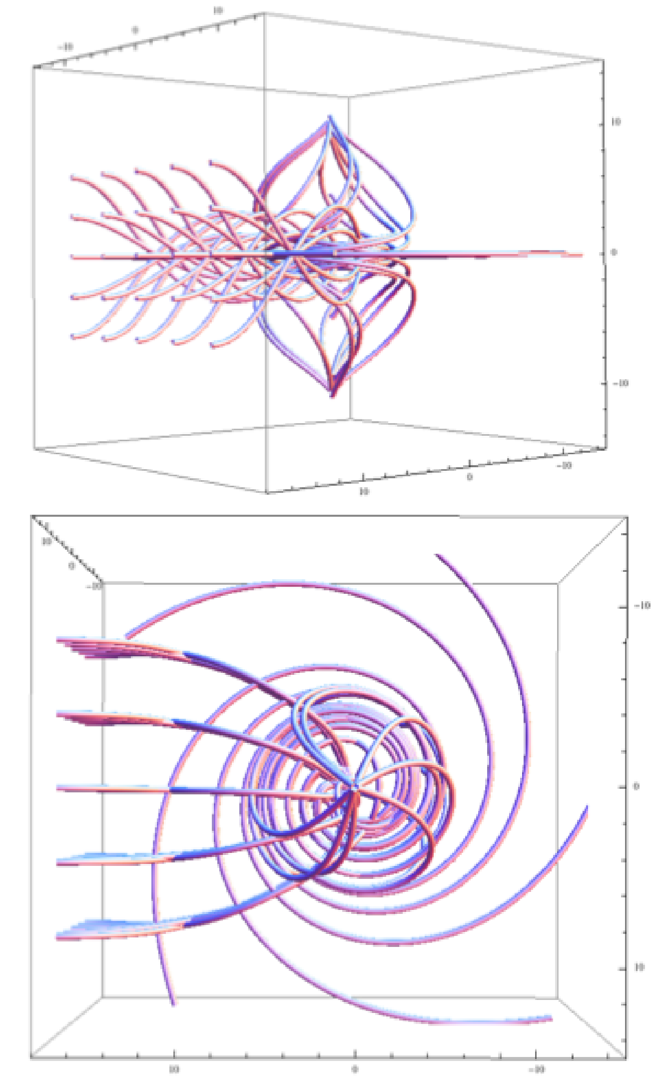

FIG. 12: 3-Dimensional plots of the space-time given by the manipulated Kerr Metric with an angular momentum; J=2 (counterclockwise); Eq. 26. The perspective of the plot on the top is perpendicular to the xy horizon where $x = 0$, and the plot on the bottom is looking down from $+z$ direction. Plots with bigger inputs are included in the Section VII.

The 3D plots on Fig. 12 help visualizing the space-time of the particular metric; Eq. 26. Only the light rays with $z = 0$ components swirl out, creating a spiral. However, light rays with $z \neq 0$ components wave in towards the center and swirl in towards the z axis and vanish as if they have reached the event horizon of a blackhole. (as in this program, not physically)

The same $dtdr$ component is entered into the flat space-time metric to further understand the role of the

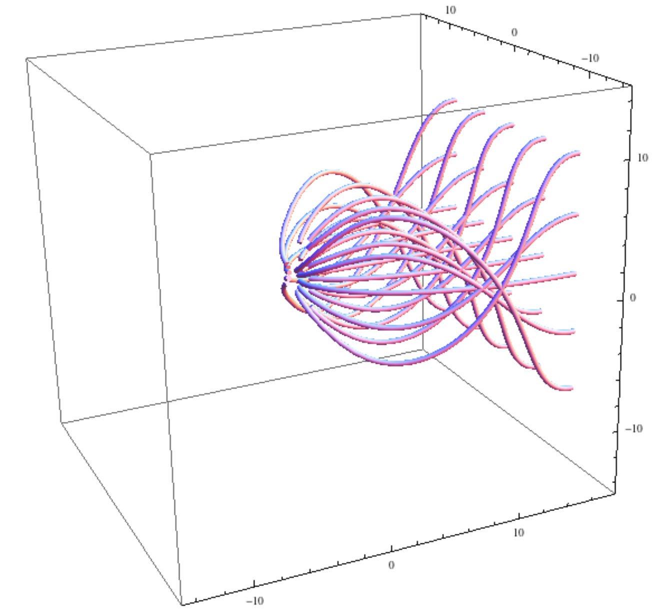

FIG. 13: 3-Dimensional plot of the space-time given by the manipulated flat space-time metric; Eq. 13.

component, resulting

$$g_{\mu\nu} \leftrightarrow \begin{bmatrix} -1 & -r\sin\theta & 0 & 0 \\ -r\sin\theta & 1 & 0 & 0 \\ 0 & 0 & r^2 & 0 \\ 0 & 0 & 0 & r^2\sin^2\theta \end{bmatrix}. \tag{27}$$

Fig. 13 is the visualization of Eq. 13. It is interesting to see that the initial behavior of the light rays are very similar to the those in Fig. 12, although the rays are driven into the event horizon in the center.

To further explore, the $d\phi d\phi$ element of the Kerr metric is added, allowing the space time to swirl. Hence, the metric will consist of the diagonal flat space-time metric elements$-(r\sin\theta dtdr)$ + ($d\phi d\phi$ element of the Kerr metric).

$$g_{\mu\nu} \leftrightarrow \begin{bmatrix} -1 & -r\sin\theta & 0 & 0 \\ -r\sin\theta & 1 & 0 & 0 \\ 0 & 0 & r^2 & 0 \\ 0 & 0 & 0 & r^2\sin^2\theta \end{bmatrix}. \tag{28}$$

The 2 dimensional visualization is shown in Fig. 14. There is no explanation for such phenomena. The bold pink and green rays shooting out from the origin seem to be numerical errors. The 3 dimensional version was not plotted, as it required more powerful computer or more efficient program.

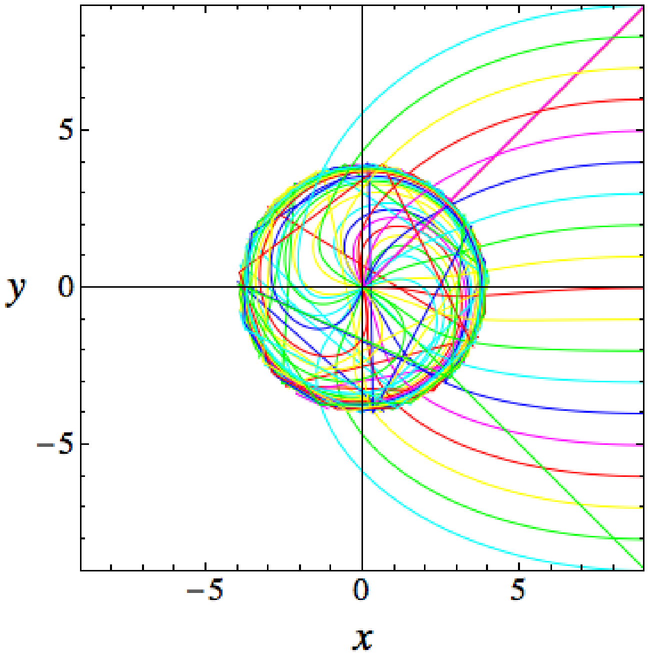

FIG. 14: 2-Dimensional plot of the space-time given by the Eq. 14. There is no explanation for the phenomena. The bold pink and green light rays shooting out from the origin are numerical errors.

V. CONCLUSION

The program capable of creating a specific space-time according to the given metric was successfully developed. The next step would be creating a program that also generates the corresponding stress energy momentum tensor to the metric given. Such program will bring us a step closer to practical space-time engineering, which will hugely assist in developing the cloaking through stress energy momentum, that has been attempted in College of Wooster physics department. (Even though the discovery of the negative energy density is required in order to develop the cloak in reality)

Moreover, visualizations that were generated through the program have their limits in explaining what exactly is happening. Also, because of the generalness of the metric that the program accepts, only having mathematical boundaries, it is hard to know the physical boundaries in terms of practical metrics.

Finally, the discovery of Eq. 26 was accidental. The space-time curvature provided by the metric is very intriguing, as it somewhat resembles the structure of spiral galaxies, although there is no evidence for the connection. Unfortunately, attempts to understand more in depth had only lead us to incomprehensible results.

[1] Breton, N., 2011, *An introduction to general relativity, black holes and gravitational waves.* (Cinvestav-IPN, Dpto. de Fisica, Apdo. 14-740, D.F., Mexico City, Mexico).
[2] Hobson, P., G. Efstathiou, and A. Lasenby, 2006, *General Relativity: An Introduction for Physicists* (Cambridge University Press), ISBN 9780521829519.
[3] Markley, L. C., and J. F. Lindner, 2013, Results in Physics **3**(0), 24 , ISSN 2211-3797.
[4] Price, D., 2012, The Ultimate Shield: Perturbing Spacetime-Summer Research .
[5] Salem, S., 2013, Spacetime: Engineering and Metaphysics-Senior Independent Study Thesis .